

JOURNAL OF THE AMERICAN CHEMICAL SOCIETY

Registered in U.S. Patent Office. © Copyright, 1976, by the American Chemical Society

VOLUME 98, NUMBER 17

AUGUST 18, 1976

Megawatt Infrared Laser Chemistry of CClF_3 and CCl_3F . 1. Photochemistry, Photophysics, and Effect of H_2 ^{1a}

David F. Dever^{1b} and Ernest Grunwald*^{1c}

Contribution from the Chemistry Department, Brandeis University,
Waltham, Massachusetts 02154. Received October 3, 1975

Abstract: 1.5 MW/cm² irradiation of 60 Torr of CClF_3 at 1090 cm⁻¹ with a pulsed CO₂ laser leads to the formation of C_2F_6 , CF_4 , and CCl_2F_2 as detected products. Conversion per flash (CPF) is as high as 1.6%. In the presence of H_2 , the principal one-carbon product becomes CHF_3 ; additional two-carbon products are C_2F_4 and C_2H_2 . Similar irradiation of 60 Torr of CCl_3F at 1079 cm⁻¹, either as the pure gas or in the presence of 0–20 Torr of H_2 , yields $\text{CCl}_2=\text{CF}_2$, and *cis*- and *trans*- $\text{CClF}=\text{CClF}$ as detected products. CPF is as high as 14%. Above 20 Torr of H_2 , formation of C_2H_2 and of a carbonaceous solid with emission of light becomes progressively more important. Optical absorption coefficients were measured for CClF_3 and CCl_3F at 60 Torr in thin cells at infrared dose levels per flash of 0.1–0.4 J/cm² (~0.5–2 MW/cm² average power). Values range from 0.25 to 0.35 of conventional low-intensity absorption coefficients. Under these conditions E_{abs} , the amount of radiant energy absorbed, ranges from 6 to 19 kcal/mol, or an average of 2–6 photons/molecule. Chemical and thermochemical considerations indicate that for CClF_3 , the primary process is C–Cl bond rupture ($E_{\text{act}} = 86 \pm 2$ kcal/mol); for CCl_3F , it is dissociation to $\text{CClF} + \text{Cl}_2$ ($E_{\text{act}} \approx 81 \pm 5$ kcal/mol). Plots of $\ln(\text{CPF})$ vs. E_{abs}^{-1} are linear, with slopes of 86 ± 4 and 81 ± 3 kcal/mol, which are practically equal to the respective values of E_{act} . Analysis of the energy distribution implied by this relationship indicates that the primary process takes place essentially while the excitation energy still resides in the vibrational mode into which it was absorbed. Rapid subsequent conversion of the excitation energy into random thermal energy produces gas phase temperatures T_m ranging up to 1200 K. Cooling of the gas phase is slow enough so that the chemical reactions subsequent to the primary process, with half-lives of 1–10 μs , take place essentially at T_m . In the present experiments the gas phase returns to room temperature prior to application of the next laser flash.

There is considerable current interest in the use of tunable infrared lasers as specific energy sources for inducing chemical reaction^{2–8} and for isotope separation in the gas phase.^{8–12} In this laboratory we have been using a tunable pulsed CO₂ laser with a typical average power output of 0.6–2 MW/cm². A high laser power is desirable in order that transitions between vibrational levels owing to interaction with the radiation field be fast compared to transitions induced by molecular collision.

In exploratory experiments in our laboratory,¹³ several dozen binary mixtures of gases were irradiated at pressures of 0.05–0.3 atm. The laser was tuned to an absorption band of one of the gaseous components and a search was made for the appearance of products. The following conclusions were reached: 1. There was a high (ca. 50%) success rate of inducing reaction. 2. The laser must be tuned to a very strong absorption band (Beer's law extinction coefficient ~0.01 Torr⁻¹ cm⁻¹ or greater). 3. Several photons are absorbed per molecule. 4. Nature and yields of reaction products vary with frequency and intensity of the radiation.

We now report a quantitative study of the infrared-laser induced reactions of CClF_3 and of CCl_3F in the gas phase, both as pure gases at 60 Torr and in the presence of 0–60 Torr of

hydrogen. In a typical experiment, we measure the infrared spectrum prior to irradiation, irradiate for 1–10 flashes, and measure the infrared spectrum again. The new absorption bands that appear permit identification of the products and determination of their partial pressures. Results were reproducible, and conversion of the reactants was in excess of 1% per flash at the higher intensities. The nature and relative amounts of the products, and the dependence of reaction yields on infrared intensity, permit us to characterize the primary decomposition and subsequent reaction steps, and to elucidate the manner in which the infrared energy is utilized.

The substrates CClF_3 and CCl_3F were chosen for study because thermochemical data (to be cited later) indicated that the modes of decomposition might be different, because both gases absorb strongly in the tunable range of the CO₂ laser, and because the related CF_2Cl_2 is known to undergo laser-induced reaction at both low^{4,5} and high¹³ infrared power levels. In our experiments, the laser was tuned to the P branch of the ν_1 absorption band. It was convenient to work at 1090 cm⁻¹ for CClF_3 and 1079 cm⁻¹ for CCl_3F . The ν_1 mode is a symmetric mode of symmetry species A_1 .^{14–17} In the case of CClF_3 , $\nu_1 = 1102$ cm⁻¹ and the mode is described essentially as a symmetric CF_3 stretching mode.¹⁶ In the case of CCl_3F ,

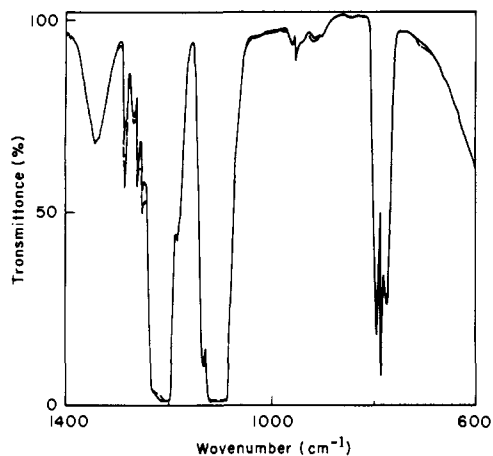


Figure 1. Before-and-after infrared spectrum for 60 Torr of CClF_3 irradiated at 1090 cm^{-1} in a 7.1-cm cell for 10 flashes. New bands (left to right) are assigned as follows: CF_4 , 1283 cm^{-1} ; C_2F_6 , 1250 cm^{-1} ; CCl_2F_2 , 1160 and 923 cm^{-1} ; C_2F_6 , 715 cm^{-1} .

$\nu_1 = 1085\text{ cm}^{-1}$ and is described essentially as a C-F stretching mode.¹⁵⁻¹⁷ Our infrared laser frequency also excites a weaker combination band, $\nu_4 + \nu_6$, of CCl_3F at 1081 cm^{-1} .¹⁷

Experimental Part

Instrumentation. The laser was a Lumonics Research Model TEA 103 tunable pulsed CO_2 laser. The radiant energy ranged from 1–3 J/pulse. Measurements with a Tachisto Model PD-1 photon drag detector indicated that about $\frac{2}{3}$ of this energy is delivered during 200 ns and most of the remainder during the subsequent 300 ns. The radiant energy was measured with a factory-calibrated Lumonics Model 20D pyroelectric detector. The calibration standard was a Scientech Disc Calorimeter. The calibration was confirmed by Dr. Hanns J. Wetzstein in our laboratory by comparison with a Gen-Tec instrument.

The laser beam was reduced to a circular area of 5.80 cm^2 by means of a lucite mask in order to eliminate outer regions of low-energy density. The energy density across the beam was examined by means of burn patterns produced on thermal recorder paper. It was never uniform, but with careful alignment of the laser the nonuniformity could be minimized. At our operating wavenumbers the energy of the unattenuated beam averaged about 0.45 J/cm^2 . When we wished to attenuate the energy, we used CaF_2 optical windows of 2, 5, or 10 mm thickness. In actinometric calculations, corrections were applied for reflection losses at interfaces.¹⁸ Flashes were repeated at 3-s intervals. Infrared wavelengths were measured with an Optical Engineering Model 16A CO_2 laser spectrum analyzer. Wavelength and energy per pulse were stable.

Optical Cells. Two kinds of cells were used, one for synthesis and the other for photophysical measurements. For synthesis, three matched cylindrical Pyrex cells of 7.1 cm length and 70 ml volume were used; the cell bodies were equipped with a vacuum stopcock, and NaCl windows were mounted vacuum tight with glypt cement (GC Electronics No. 90-2).

For the photophysics measurements, a stainless steel cell with Teflon liner which defined an optical path by holding the NaCl windows 0.39 cm apart was used. O-rings provided a vacuum-tight seal between the windows and the body of the cell. The cross-sectional area of the cell was 8.04 cm^2 . In view of the 5.80-cm^2 cross section of the laser beam, this defines a radiation-filling factor of 0.72.

Air leaks into the optical cells were readily detected because irradiation of CClF_3 and CCl_3F in the presence of O_2 leads to the formation, respectively, of COF_2 and COCIF , which have a strong and unobscured absorption band at or near 1930 cm^{-1} .

Reagents. Gaseous CClF_3 , and research purity H_2 were obtained from Matheson Gas Products in lecture bottle quantities and were used without further purification. CCl_3F was obtained from Wilmod Glass Co., Buena, N.J. and the liquid was degassed and distilled below dry-ice temperature. Other materials used for obtaining standard spectra were obtained either from Matheson Gas Products or from

Table I. Optical Extinction Coefficients in the Gas Phase

Compd	$\bar{\nu}$, cm^{-1}	Extinction coefficient, $\text{cm}^{-1}\text{ Torr}^{-1}$
CClF_3	1090	0.0189
CCl_3F	1079	0.0135
CF_4	1282	0.14
CHF_3	700	0.0026
CCl_2F_2	922	0.034
$\text{CCl}_2=\text{CF}_2$	1740	0.0087
	1325	0.0081
$\text{CF}_2=\text{CF}_2$	1344	0.065
	1180	0.068
C_2F_6	1250	0.10
	716(s)	0.0023 ^a
<i>cis</i> - $\text{CClF}=\text{CClF}$	1168	0.020 ^b
	958	0.010 ^b
<i>trans</i> - $\text{CClF}=\text{CClF}$	1218	0.018 ^b
	894	0.012 ^b
$\text{HC}\equiv\text{CH}$	730(s)	0.017 ^a
HCl(P3)	2821	0.00042

^a Spike only. ^b N. C. Craig and D. A. Evans, *J. Am. Chem. Soc.*, **87** 4223 (1965).

PCR Inc., Gainesville, Fla. Standard manometric vacuum-line techniques were used in filling the cells.

Analytical Techniques. Reactant disappearance and product appearance were monitored by before-and-after ir scans using a Perkin-Elmer Model 567 Spectrometer. Criteria for product identification were (1) all unobscured strong bands must be present, and (2) the bands must have the correct frequency, shape, and relative intensities. Whenever possible, ir spectra of authentic samples were recorded under identical instrumental conditions and had to give perfect overlays.

By meeting these criteria, we feel confident that the identifications made are correct, especially since authentic samples were available in all but two cases. Moreover, we feel that identification of ir-active products is reasonably complete, because all new absorption bands could be assigned.

Partial pressure of products were calculated from optical densities at suitable wavelengths. Pertinent extinction coefficients are listed in Table I. To the accuracy desired ($\pm 10\%$), and at the relatively low pressures employed (60–120 Torr), it was not deemed worthwhile to make corrections for pressure broadening.¹⁹

Results

Products from CClF_3 . Figure 1 is representative of data collected in a typical experiment. All new bands can be assigned to the following products: CF_4 , 0.075 Torr/flash; C_2F_6 , 0.068 Torr/flash; CCl_2F_2 , 0.039 Torr/flash. The rate of disappearance of CClF_3 could not be followed accurately. A rough estimate is -0.2 Torr/flash; from the amount of detected products, we would expect to see -0.25 Torr/flash. This, coupled with the fact that there are no unassigned peaks in the "after" spectrum, lets us be confident that we have identified most if not all infrared-active major products. Products will be missed only if they are infrared inactive (such as Cl_2), if they lack strong infrared absorption bands, or if all strong absorption bands happen to be obscured.

There was no evidence for carbon formation, nor was there evidence for the emission of visible light flashes or scintillations from the reaction cell.

Products from $\text{CClF}_3 + \text{H}_2$. The addition of hydrogen increases the reaction rate and modifies the products. The yields of CF_4 and CCl_2F_2 drop drastically; that of C_2F_6 increases at low hydrogen pressures, reaches a maximum near $P_{\text{H}_2} = 10$ Torr, and then decreases gradually. New products are CHF_3 , $\text{CF}_2=\text{CF}_2$, C_2H_2 , HCl , and HF . The latter is detected as SiF_4 in a glass cell.

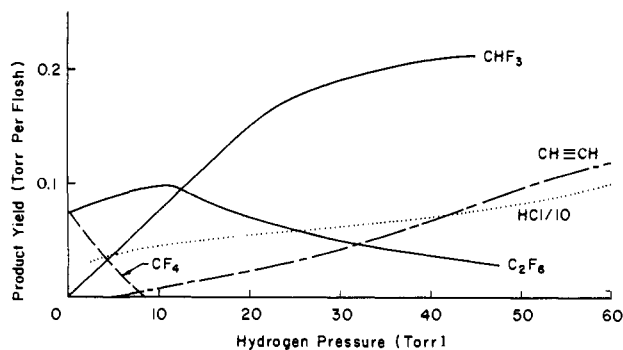


Figure 2. Representative product yields, in Torr/flash, as a function of H₂ pressure for 60 Torr of CCl₃F in a 7.1-cm cell.

Yields per flash in the photolysis of 60 Torr of CCl₃F are shown in Figure 2 as a function of hydrogen pressure. Of special interest is the curve for HCl, which measures the total reaction rate; the relative yields of CF₄ and CHF₃, which may result from alternate reactions of CF₃ radical intermediates; and the yield of C₂F₆, which indicates the rather high concentrations of CF₃ radicals produced in each flash. The fraction [C₂F₄]/([C₂F₄] + [C₂F₆]) is approximately proportional to the hydrogen pressure, increasing from 0.00 at 0 Torr to 0.32 at 14 Torr, to 0.78 at 45 Torr. The yield of CCl₂F₂ decreases rapidly with hydrogen pressure, being reduced by more than one order of magnitude at 10 Torr.

Products from CCl₃F. Figure 3 shows a typical "before and after" spectrum. All new bands can be assigned to the following products: *cis*-CClF=CClF, 0.12 Torr/flash; *trans*-CClF=CClF, 0.12 Torr/flash; CCl₂=CF₂, 0.04 Torr/flash. The rate of disappearance of CCl₃F was found to be -0.6 ± 0.1 Torr/flash. From the amounts of detected products, we would have expected -0.56 Torr/flash. Stoichiometry requires the formation of 1 mol of Cl₂/mol of CCl₃F reacting. Cl₂ is infrared inactive; however, in the presence of H₂ a roughly equivalent amount (ca. 1.5 Torr) of HCl is produced. There is no evidence for the formation CF₂Cl₂, CCl₄, CCl₂FCCl₂F, or carbon, nor for the emission of visible light during photolysis.

Products from CCl₃F + H₂. The effect of H₂ on the laser-induced reaction of CCl₃F is quite different from that on the reaction of CClF₃. In the following, it will be convenient to give separate descriptions of the effects of low (<20 Torr) and of moderate (20–60 Torr) hydrogen pressures. The CCl₃F pressure is 60 Torr throughout.

At low hydrogen pressures, there is a marked increase in the reaction rate, yet there appear no new products. In particular, there is no evidence for the formation of compounds with C–H

bonds, such as CHFCl₂. The percent conversion of CCl₃F per flash increases approximately linearly with hydrogen pressure, being 5–6 times greater at 20 Torr of H₂ than in the absence of hydrogen. The relative yields of CF₂=CCl₂/*cis*-C₂Cl₂F₂/*trans*-C₂Cl₂F₂ (which are 0.33/1/1 in the absence of H₂) increase in the ratio of 1.3/1/1, so that at 20 Torr of H₂, the three isomers are produced in nearly equal amounts. There is no evidence of carbon formation and no visible light emission.

Above 20 Torr of H₂, the reaction changes significantly. At 35 Torr one observes a darkening of the cell walls due to the deposition of a carbonaceous solid, as well as a bluish-orange emission whose peculiar character may have been the combined effect of a bluish fluorescence and a more slowly emitted carbonaceous incandescence. At 60 Torr of H₂ there appears a brilliant bright-orange flame throughout the cell, whose brilliance diminishes with successive flashes and which becomes a faint scintillation after about 15 flashes. The chemical changes which occur in this region are indicated in Figure 4. Between 35 and 40 Torr of H₂, there is a rapid increase in HCl formation and a concomitant rapid increase in C₂H₂ formation, while the formation of the C₂Cl₂F₂ isomers becomes quenched. There is also a detectable trace of CCl₂F₂. Above 40 Torr there is a generalized quenching of gaseous product formation.

Quenching. An exploratory study of the effect of added gases was made and the anticipated quenching of laser-induced reaction was observed. For instance, in the photolysis of 60 Torr of CCl₃F + 60 Torr of H₂, the yield of *trans*-C₂Cl₂F₂ per flash is reduced to 57 and 37% respectively by the addition of 26 and 60 Torr of HCl; the yield is reduced to 31 and 26% respectively by the addition of 62 and 81 Torr of argon.

Evidence for specific quenching by reaction products may be inferred from the fact that the percent conversion per flash in some cases decreases as reaction progresses.

Photophysical Studies. At the high infrared intensities characteristic of our laser output, one may expect deviations from the Beer-Lambert law owing to optical saturation and multiple photon absorption. Absorption coefficients were measured with a pyroelectric detector at typical reaction intensities in an 0.39-cm cell. Under these conditions, 20–30% of the incident energy is absorbed.

We define $\alpha = l^{-1} \log (D_0/D)$, where D denotes mean dose/cm² ($\int I dt/A$) per flash. By virtue of this definition, α reduces simply to $\alpha_0 = l^{-1} \log (I_0/I)$, the conventional optical density per centimeter, in the low-intensity limit where the Beer-Lambert law is valid throughout the flash. Experimental results are listed in Table II. It can be seen that α ranges from 0.25 to 0.35 of α_0 . The latter is measured with an infrared spectrophotometer in the normal way.

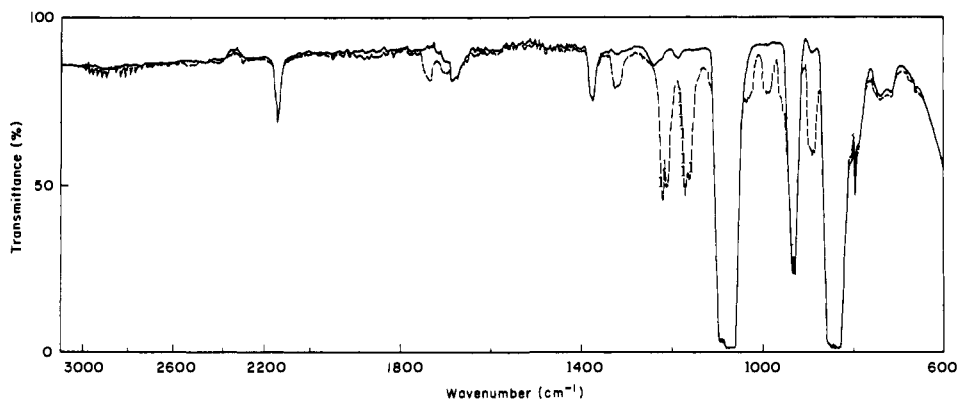


Figure 3. Before-and-after infrared spectrum for 60 Torr of CCl₃F + 1.5 Torr of H₂ irradiated at 1079 cm⁻¹ in a 7.1-cm cell for 10 flashes. New bands (left to right) are assigned as follows: HCl, 3040–2700 cm⁻¹; CF₂=CCl₂, ~1740 and ~1320 cm⁻¹; *trans*-C₂Cl₂F₂, 1220 and 1210 cm⁻¹; *cis*-C₂Cl₂F₂, 1170 and 1160 cm⁻¹; CCl₂=CF₂, ~1030 and 988 cm⁻¹; *cis*-C₂Cl₂F₂, ~960 cm⁻¹; *trans*-C₂Cl₂F₂, ~890 cm⁻¹.

Table II. Photophysics and Effect of Absorbed Energy on Percent Conversion per Flash

No.	D , J/cm ²	α , cm ⁻¹	E_{abs} in 0.39-cm cell		CPF, %
			kcal/mol	photons/molecule	
(a) CClF ₃ (60 Torr) at 1090 cm ⁻¹					
1	0.309	0.340	18.6	6.0	1.58
2	0.215	0.358	13.6	4.4	0.374
3	0.200	0.343	12.0	3.8	0.120
4	0.125	0.373	8.4	2.7	0.0060
	0	1.13			
(b) CCl ₃ F (60 Torr) at 1079 cm ⁻¹					
5	0.372	0.199	13.3	4.3	2.8
6	0.270	0.232	11.2	3.6	0.80
7	0.230	0.242	9.9	3.2	0.40
8	0.135	0.284	6.9	2.2	0.009
	0	0.808			
(c) CCl ₃ F (60 Torr) + H ₂ (20 Torr) at 1079 cm ⁻¹					
9	0.385	0.203	14.0	4.5	14.4(10.6) ^a
10	0.276	0.206	10.2	3.3	2.0(1.6)
11	0.217	0.216	8.4	2.7	0.53(0.45)
12	0.133	0.256	6.1	2.0	0.008(0.006)
	0	0.808			
(d) Least-Squares Analysis ^b					
1-4 $\ln(\text{CPF}) = (5.14 \pm 0.30) - (85.8 \pm 4.1)/E_{\text{abs}}$; $r = 0.995$					
5-8 $\ln(\text{CPF}) = (7.12 \pm 0.25) - (81.1 \pm 2.7)/E_{\text{abs}}$; $r = 0.997$					
9-12 $\ln(\text{CPF}) = (8.36 \pm 0.49) - (78.7 \pm 4.9)/E_{\text{abs}}$; $r = 0.992$					
9-12 $\ln(\text{addnl CPF}) = (7.93 \pm 0.60) - (78.9 \pm 6.1)/E_{\text{abs}}$; $r = 0.987$					

^a Figures in parentheses denote *additional* CPF owing to added 20 Torr of hydrogen. ^b r denotes the statistical correlation coefficient.

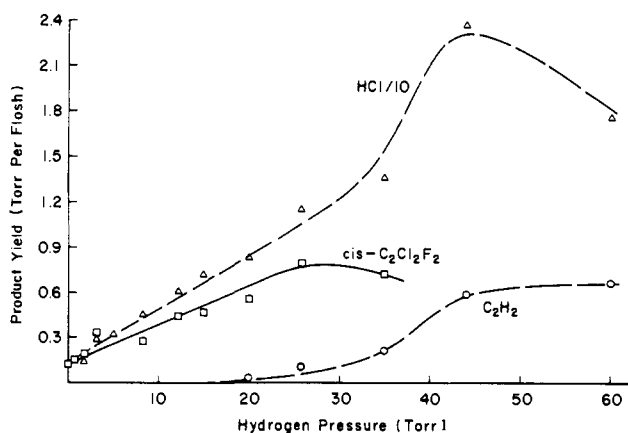


Figure 4. Representative product yields, in Torr/flash, as a function of H₂ pressure for 60 Torr of CCl₃F in a 7.1-cm cell.

On a purely empirical basis, the absorption coefficients can be represented by eq 1, where B and n are adjustable constants.

$$\alpha = \alpha_0 / (1 + BD^n) \quad (1a)$$

$$-dD/dl = 2.303D\alpha_0 / (1 + BD^n) \quad (1b)$$

The following values fit our data: for CClF₃, $\alpha_0 = 1.13$, $B = 2.80$, $n = 0.15$; for CCl₃F, $\alpha_0 = 0.81$, $B = 4.53$, $n = 0.4$. The differential form of eq 1b is convenient for calculating the absorbed-energy profile in longer cells.

Effect of Absorbed Energy on Reaction Rate. The same 0.39-cm cell used for the photophysical measurements was also used to measure the sensitivity of the reaction rate to absorbed energy. The laser was adjusted carefully for maximum uniformity of dose across the beam, the standard deviation being within 30%. In view of the nonlinear form of (1b), the resulting standard deviation in E_{abs} , the amount of energy absorbed, is within 15%.

Experimental results are included in Table II. E_{abs} is expressed both in kcal/mol and photons/molecule. CPF denotes conversion per flash and is expressed in percent of reactant. Measurements were made for (a) 60 Torr of CClF₃, (b) 60 Torr of CCl₃F, and (c) 60 Torr of CCl₃F + 20 Torr of H₂. The amount of energy absorbed ranges from 2 to 6 photons per molecule. CPF changes by three orders of magnitude and is as high as 14% per flash. The amount of radiation used to measure CPF ranged from 1 to 500 flashes. It had been shown in separate experiments, at low conversions, that CPF is constant. The 5–15% decrease of the reactant could be measured with fair accuracy by absorbance peaks that were not complicated by product absorption.

Discussion

Our results encourage the hope that a high-energy chemistry based on vibrational excitation of specific substances with high-power infrared lasers will be efficient, controllable, and selective. The photophysical measurements show that absorption coefficients do not decrease drastically at high intensities. Thus, substantial amounts of energy, amounting to several photons per molecule, are absorbed. The resulting degrees of conversion, though sensitive to the amount of energy absorbed, reach more than 10% per flash. By repeating the flashes, one obtains synthetically useful build-up of products. Normally unreactive substances, such as the Freons used in this study, can be activated to give products.

The marked differences in the reaction products of CClF₃ and CCl₃F indicates that the laser-induced chemistry is highly selective. For CClF₃, the products are typical of a free-radical mechanism involving the formation of CF₃· as the first step. For CCl₃F, we suggest that the primary process is the formation of the carbene :CClF.

In suggesting reaction mechanisms for laser-induced reactions, it is useful to keep in mind both chemical and thermochemical considerations. Because vibrational excitation leaves the molecules in their electronic ground states, the chemistry

Table III. ΔH° for Various Reactions Involving CClF_3

Reaction	ΔH°_{298} , kcal ^a
(R1) $\text{CClF}_3 \rightarrow \text{CF}_3 + \text{Cl}$	86
(R2) $\text{CClF}_3 \rightarrow \text{CClF}_2 + \text{F}$	124
(R3) $\text{CClF}_3 \rightarrow \text{CF}_2 + \text{FCl}$	106
(R4) $\text{CF}_3 + \text{CClF}_3 \rightarrow \text{CF}_4 + \text{CClF}_2$	-6
(R5) $\text{CClF}_2 + \text{CClF}_3 \rightarrow \text{CCl}_2\text{F}_2 + \text{CF}_3$	3
(R6) $2\text{CF}_3 \rightarrow \text{C}_2\text{F}_6$	-97
(R7) $\text{CF}_3 + \text{Cl} \rightarrow \text{CClF}_3$	-86
(R8) $2\text{Cl} \rightarrow \text{Cl}_2$	-58
(R9) $\text{CClF}_2 + \text{CF}_3 \rightarrow \text{CF}_3\text{CClF}_2$	-91
(R10) $\text{CF}_3 + \text{H}_2 \rightarrow \text{CF}_3\text{H} + \text{H}$	-3
(R11) $\text{CClF}_3 + \text{H} \rightarrow \text{CF}_3 + \text{HCl}$	-17
(R12) $\text{C}_2\text{F}_6 \rightarrow \text{C}_2\text{F}_4 + \text{F}_2$	164
(R13) C_2F_6 (97 kcal) + $\text{H}_2 \rightarrow \text{C}_2\text{F}_4 + 2\text{HF}$	-63

^a The following values of ΔH_f° were used: gas, ΔH_f° in kcal/mol; CClF_3 , -169; CF_3 , -112; CClF_2 , (-64); CF_2 , -44; F , 19; Cl , 29; FCl , -19; CF_4 , -223; CCl_2F_2 , -118; C_2F_6 , -321; C_2F_4 , -157; CF_3H , -167; H , 52; HCl , -22; HF , -65. Values in parentheses were estimated by us.

may be interpreted in terms of familiar high-temperature thermal reaction mechanisms. The thermochemistry indicates sine qua non conditions: a positive value of ΔH° will set a lower limit to the required thermal activation energy; a negative value of ΔH° will set a lower limit to the amount of excitation energy resulting in the products.

In the following discussion it will be convenient to use values of ΔH° at 298 °C. Although the populations of energy levels during and right after the laser flash are enormously different from equilibrium Boltzmann distributions, the systems are initially at 298 °C and return essentially to 298 °C during the 3-s intervals between laser flashes. Moreover, for many of the species to be considered, the uncertainties in the required enthalpies of formation, ΔH_f° , are far greater than the variation of ΔH° within the temperature range of interest. Values of ΔH_f° were taken from the JANAF Tables²⁰ and from tabulations by Cox and Pilcher, and Benson.²¹ When experimental values were not available, required values were estimated by interpolation, using essentially the methods described by Benson.^{21b} Such estimates will be listed in parentheses in footnotes of Tables III and IV.

Reactions of CClF_3 . Thermochemical data for reactions of interest are listed in Table III. Reactions R1–R3 show possible modes of decomposition. (R1) clearly has the smallest ΔH° , and the products indicate that this is indeed the primary process. The halogen-abstraction reactions R4 and R5 then account for the formation of CF_4 and CCl_2F_2 , while (R6) accounts for that of C_2F_6 . For consistency with (R6), we must assume that (R7), which reverses the primary process, and (R8) are also significant. Moreover, the fact that the yield of CCl_2F_2 is smaller than that of CF_4 suggests that CClF_2 radicals formed in (R4) also react other than by (R5). The most likely process is (R9); however, the expected very strong absorption band of CClF_2CF_3 at $\sim 1115 \text{ cm}^{-1}$ is obscured by CClF_3 absorption (Figure 1).

Formally, the sequence of reactions R1 plus R4–R8 is a chain reaction. However, the yields of CF_4 and CCl_2F_2 are not large compared to that of C_2F_6 , indicating that the concept of a chain reaction must be abandoned and that the concentrations of CF_3 radicals are high enough to promote bimolecular radical combination. Indeed, judging by the amount of C_2F_6 produced, the CF_3 concentrations attained during the flash may well be as high as 0.1 Torr.

According to thermochemical data, the C_2F_6 molecules produced according to (R6) have a minimum internal energy

Table IV. ΔH° for Various Reactions Involving CCl_3F

Reaction	ΔH°_{298} , kcal ^a
(R14) $\text{CCl}_3\text{F} \rightarrow \text{CCl}_2\text{F} + \text{Cl}$	77
(R15) $\text{CCl}_2\text{F} + \text{CCl}_3\text{F} \rightarrow \text{CCl}_2\text{F}_2 + \text{CCl}_3$	-9
(R16) $\text{CCl}_3 + \text{CCl}_3\text{F} \rightarrow \text{CCl}_4 + \text{CCl}_2\text{F}$	6
(R17) $\text{CCl}_2\text{F} + \text{H}_2 \rightarrow \text{HCCl}_2\text{F} + \text{H}$	4
(R18) $\text{H} + \text{CCl}_3\text{F} \rightarrow \text{HCl} + \text{CCl}_2\text{F}$	-26
(R19) $\text{CCl}_3\text{F} \rightarrow \text{CClF} + \text{Cl}_2$	78
(R20) $\text{CClF} + \text{CCl}_3\text{F} \rightarrow \text{C}_2\text{Cl}_4\text{F}_2$ (1,1 or 1,2)	ca. -58
(R21) $\text{C}_2\text{Cl}_4\text{F}_2^*$ (58 kcal) $\rightarrow \text{C}_2\text{F}_2\text{Cl}_2$ (1,1; <i>cis</i> -1,2; or <i>trans</i> -1,2) + Cl_2	ca. -18
(R22) $\text{CClF} + \text{Cl}_2 \rightarrow \text{CCl}_3\text{F}$	-78
(R23) $\text{Cl}_2 + \text{H}_2 \rightarrow 2\text{HCl}$	-44
(R24) $\text{CCl}_3\text{F} + \text{H}_2 \rightarrow \text{CClF} + 2\text{HCl}$	34
(R25) $\text{C}_2\text{Cl}_4\text{F}_2^*$ (58 kcal) + $\text{H}_2 \rightarrow \text{C}_2\text{F}_2\text{Cl}_2 + 2\text{HCl}$	ca. -62

^a The following values (in kcal/mol) of ΔH_f° were used: $\text{CCl}_3\text{F}(\text{g})$, -69; CCl_2F , (-21); CClF , (9); CCl_2 , 57; CCl_3 , 19; $(\text{CCl}_2\text{F})_2$, (-118); $\text{C}_2\text{F}_2\text{Cl}_2$ (any isomer), -76 to -78; HCCl_2F , -69. See also footnote of Table III.

of 97 kcal/mol. Apparently, this is not sufficient to permit spontaneous decomposition to C_2F_4 , in spite of the favorable entropy change ($\Delta S^\circ_{298} = 41$ gibbs, $\Delta H^\circ_{298} = 164$ kcal). No C_2F_4 was detected. When H_2 is added, a new reaction sequence ensues, involving (R10) and (R11) as propagation steps. Substantial yields of CF_3H are obtained, and the yields of CF_4 and C_2F_6 drop off (Figure 2). The activation energy for H abstraction according to (R10), 10 ± 1 kcal,²² evidently is considerably lower than that for F abstraction according to (R4). Activation energies for the competing radical combination reactions, such as (R6), (R7), and (R9), are close enough to zero to be negligible for our purposes.²²

The addition of H_2 also leads to the formation of C_2F_4 . Since the fraction $[\text{C}_2\text{F}_4]/([\text{C}_2\text{F}_4] + [\text{C}_2\text{F}_6])$ is roughly proportional to the hydrogen pressure, it is possible that C_2F_4 is produced in a direct bimolecular reaction (reaction R13) between H_2 and vibrationally excited C_2F_6 . The thermochemistry for this process would be favorable owing to the formation of two HF bonds.

In conclusion, a free-radical mechanism with (R1) as initiating step can account for all known products except acetylene, whose mode of formation is obscure. However, $\text{HC}\equiv\text{CH}$ is often formed under pyrolytic conditions. Under the stated conditions there were no detectable amounts of the following potential products: CHClF_2 , dihalomethylenes, and 1,1,2,2-tetrafluoroethane.

Reactions of CCl_3F . Thermochemical data for reactions of interest are listed in Table IV. This time there are two potentially favored modes of decomposition with nearly equal ΔH° : C–Cl bond rupture (reaction R14) and CClF carbene formation (reaction R19), both of which proceed with $\Delta H^\circ_{298} \approx 78$ kcal. Decompositions into $\text{CCl}_3 + \text{F}$ or into $\text{CCl}_2 + \text{ClF}$ are associated with $\Delta H^\circ_{298} \approx 107$ kcal and are relatively improbable.

Of the two potentially favored modes of decomposition, the nature of the reaction products indicates that free-radical decomposition is not a major mode. In particular, there is no detectable formation of CCl_2F_2 , CCl_4 , or $\text{CCl}_2\text{FCCl}_2\text{F}$. On the basis of energetics, and by analogy with reaction products obtained from CClF_3 (compare (R15) and (R16) with (R4) and (R5)), such products would have been expected. In the presence of H_2 there is no detectable formation of HCCl_2F , in spite of the analogy of (R17) + (R18) to (R10) + (R11). We estimate that the activation energy for (R17) is higher than that for (R10) by 3–4 kcal. This difference should not be prohibitive at the high temperatures involved.

Accepting (R19) as the primary decomposition step, we may postulate that the actual products, the three isomers of $C_2Cl_2F_2$, are formed by insertion of the carbene $CClF$ into a C-Cl or C-F bond, (R20). The resulting perhaloethane molecules have enough internal energy to eject Cl_2 , yielding the product olefin, (R21). There is some precedent for the insertion of dihalocarbenes into polar bonds in liquid solution,^{23a} but we are not familiar with close analogues of the specific process we envisage in the gas phase.^{23b}

Since (R19) takes preference over (R14), it is not likely that the activation energy for (R19) is much greater than that for (R14). The latter is a simple bond dissociation for which one may expect that $E_{act} \approx \Delta H^\circ$.^{24a} (R19) is a three-center elimination for which, in the only analogue known to us, E_{act} is greater than ΔH°_{298} by 3 ± 2 kcal;^{24b} we shall therefore adopt the value $E_{act} = 81$ kcal for (R19). As a corollary, E_{act} for the reverse process, (R22), will be only 3 kcal. Thus reversal of the primary process according to (R22) may be kinetically significant compared to product formation according to (R20) + (R21).

The apparent preference of (R19) over (R14), in spite of the slightly greater thermal activation energy, illustrates that reaction paths may be different when activation is by absorption of energy into a specific vibrational mode rather than by random thermal excitation.

The addition of H_2 causes a marked increase in the rate of product formation and increases the relative proportion of $CCl_2=CF_2$. The increased yield may result indirectly from the reaction of H_2 with Cl_2 , (R23), which removes Cl_2 from the reaction mixture and thus reduces the importance of the back-reaction, (R22). Calculations made in a later section will show that, owing to the exothermicity of (R23), the effective temperature actually rises when H_2 is added, which may explain the increase in the relative proportion of $CCl_2=CF_2$ in the product.

An alternative explanation would have H_2 participate directly in the primary process according to (R24). This would reduce ΔH° by 44 kcal relative to that for (R19), and it is conceivable that there would also be a substantial lowering of the activation energy. In the preceding section, to account for the formation of C_2F_4 in the presence of H_2 , the theory was proposed that H_2 promotes halogen elimination from vibrationally excited halocarbons. (R24) could be a further instance of this phenomenon. For consistency, H_2 would then also promote halogen elimination from vibrationally excited $C_2Cl_4F_2$, as indicated in (R25), and this may somehow account for the increased proportion of $CCl_2=CF_2$ in the product.

At moderate hydrogen pressures (20–60 Torr), the reaction becomes more complicated. There are now substantial quantities of pyrolysis products, particularly of acetylene and carbon. There are also trace amounts of CF_2Cl_2 , indicating that free-radical mechanisms are no longer quite negligible.

Utilization of Absorbed Energy. On the basis of the reaction products there is little doubt that the primary processes are (R1) and (R19), respectively. Since the activation energies for the reverse processes are small, the thermochemistry enables us to make fairly reliable estimates, 86 and 81 kcal, respectively, for the activation energies of the primary processes.

By comparison, the average energy absorbed per mole of reactant is less than 20 kcal/mol (Table II). We shall assume that the photon energy, after absorption into the given vibrational mode, rapidly moves up and down the vibrational ladder so that a near-Boltzmann distribution is maintained in the absorbing mode throughout the laser flash. This model seems reasonable for two reasons. (1) For an ensemble of harmonic quantum oscillators, selection rules for absorption of radiation are such that, if the initial energy distribution in the absorbing mode is a Boltzmann distribution, the final distribution will also be a Boltzmann distribution. For real molecules one would

expect at least a vestige of such behavior. (2) Cross sections for collisional energy transfer within a given vibrational mode are so high that one may expect half-times for relaxation to a Boltzmann distribution within the absorbing mode to be short compared to half-times of the laser flashes, under our conditions.²⁵

Energy will also flow into other modes, at a rate whose relationship to the rate of decomposition we now wish to explore. It is convenient to examine this relationship first in crude, zeroth approximation, and then in higher approximation.

Zeroth Approximation. For definiteness, let us begin by assuming that decomposition takes place while the energy still resides in the single mode that has been excited, and that the rate constant for unimolecular decomposition is given by an Arrhenius-type relationship (eq 2). The factor $\exp(-E_{act}/RT_{osc})$ expresses the fraction of molecules whose energy in the given mode is at least E_{act} kcal/mol above the zero-point energy.

$$k = A \exp(-E_{act}/RT_{osc}) \quad (2)$$

Owing to the high energy content after irradiation, the energy-rich mode will, in zeroth approximation, behave like a classical oscillator. That is, the equipartition principle applies and the mean energy per mole of oscillators is equal to RT_{osc} . Now the mean energy per mole of oscillators = $E_{abs} + E_{initial}$, where E_{abs} is the mean energy absorbed from the radiation field per mole of oscillators, and $E_{initial}$ is the initial energy per mole in the given mode. The latter will be negligible compared to E_{abs} because the oscillator is initially at 298 K. Thus, for the given mode, $RT_{osc} = E_{abs}$, and eq 2 may be rewritten in the convenient form (3) for a primary process in which the energy still resides in the mode into which it was absorbed.

$$\ln k = \ln A - E_{act}/E_{abs} \quad (3)$$

Next, let us consider that prior to the primary process, the excitation energy is dispersed effectively into n quasi-classical modes. Then $E_{abs} = nRT_{osc}$, and eq 2 may be rewritten in the form of (4). If the effective temperatures of the n modes are unequal, or if RRKM quantum statistics²⁶ apply, we may still write an equation of the form of (4), in which n is a function whose value is greater than 1.

$$\ln k = \ln A - nE_{act}/E_{abs} \quad (4)$$

According to (3), the plot of $\ln k$ vs. E_{abs}^{-1} is linear, with a slope equal to E_{act} . According to (4), the slope (which may vary with E_{abs}) is equal to nE_{act} . Thus, if E_{act} is known, n can be evaluated and the question of whether or not the primary process takes place before the excitation energy is dispersed into other modes can be answered.

In probing this matter, we used the data in Table II, adopting CPF (conversion per flash) as a measure of k . The actual relationship that was tested is (5), in which A' and E_{act}' are empirical parameters obtained by least-squares adjustment.

$$\ln(\text{CPF}) = \ln A' - E_{act}'/E_{abs} \quad (5)$$

The variation of $\ln(\text{CPF})$ with E_{abs}^{-1} for each of the three data sets is linear with good correlation coefficient; see Table II. For the experiments without added H_2 , results are as follows: For $CClF_3$, $E_{act}' = 86 \pm 4$ kcal; $E_{act} = 86 \pm 2$ kcal; $n = 1.00 \pm 0.05$. For CCl_3F , $E_{act}' = 81 \pm 3$ kcal; $E_{act} = 81 \pm 5$ kcal; $n = 1.00 \pm 0.07$.

Higher Approximation. The results in zeroth approximation indicate, with remarkable precision, that $n = 1$. The following critique will show that this result may not be precisely correct, but should not be far wrong, either. First, the absolute accuracy of our actinometry is probably no better than 10%. Second, we are assuming that k is proportional to CPF. This may not be

exact owing to the probability that back-reaction R7 or R22 is kinetically significant. In the case of CCl_3F , it seemed possible to suppress the back-reaction R22 by doing the measurements in the presence of H_2 , so that Cl_2 becomes converted to HCl . Results of such measurements are included as No. 9–12 in Table II. The data are adequately represented by (5), with slope $E_{\text{act}}' = 79 \pm 5$ kcal, in essential agreement with $E_{\text{act}} = 81 \pm 5$ kcal, and thus giving added support to the conclusion that $n = 1$. However, even this experiment is somewhat equivocal, owing to the possibility that in the presence of H_2 part of the primary process proceeds via (R24). The theory leading to eq 3 does not apply to bimolecular reactions, such as (R24), in which only one of the reactants absorbs energy from the laser beam. The empirical eq 5 might still fit, however, except that E_{act}' then bears no simple relationship to E_{act} .

Finally, we are assuming that the excited oscillator behaves classically; i.e., $E_{\text{abs}} = RT_{\text{osc}}$. For the harmonic quantum oscillator, the corresponding relationship is (6), where $x = h\nu_{\text{osc}}/kT_{\text{osc}}$.

$$E_{\text{abs}} = RT_{\text{osc}}X \exp(-x)/[1 - \exp(-x)] \quad (6)$$

In Table V, values of E_{abs}/R are compared with values of T_{osc} computed according to (6) for the experiments listed as No. 1–4 in Table II. The plot of $\ln(\text{CPF})$ vs. $(RT_{\text{osc}})^{-1}$ is adequately linear, with slope of -106 ± 7 kcal (Table V, footnote b). Thus, to the harmonic quantum-oscillator approximation, $E_{\text{act}}' = 106 \pm 7$ kcal, $E_{\text{act}} = 86 \pm 2$ kcal, and $n = 1.23 \pm 0.09$. Within the framework of our model, the result implies that primary decomposition takes place while a fraction $1/n$, $\sim 80\%$, of the absorbed energy resides in the original mode of excitation.

Comparison with RRKM Theory. The preceding results indicate that the energy distribution of the laser-activated reacting molecules is quite different from that expected according to RRKM statistics.²⁶ For the reaction of CClF_3 , prediction according to RRKM theory is relatively simple owing to the simple C–Cl bond-breaking reaction mechanism. Briefly, in our calculations we used the known fundamental vibration frequencies of CClF_3 and assumed that in the transition-state complex, the C–Cl stretching mode becomes translation along the reaction coordinate. For each E_{abs} we then calculated the vibrational temperature (T_{vib}), assuming a Boltzmann distribution of E_{abs} among all vibrational modes. Using this temperature and an activation energy of 86 kcal, we then applied RRKM statistics to calculate k/A , where k is the macroscopic rate constant and A is an unknown, temperature-independent constant. The results were then plotted in the form of a graph of $\ln(k/A)$ vs. $1/E_{\text{abs}}$ and the average slope of the resulting slightly curved relationship determined. This slope, in the range covered by our experiments, was -296 kcal, clearly inconsistent with the experimental slope of -86 kcal. Thus, in terms of eq 4, RRKM statistics would predict an effective \bar{n} of 3.4 for the CClF_3 reaction. In view of the acknowledged success of RRKM theory in accounting for numerous thermal reactions, we note that the dynamical behavior of molecules may be quite different from that assumed by RRKM theory when activation takes place in the intense, coherent radiation fields characteristic of megawatt laser flashes.

Temperature Rise. Because some of the reaction products, especially acetylene and carbon, suggest that pyrolysis may be occurring to some extent, it is of interest to estimate the temperature rise when the absorbed energy is converted into random thermal energy. As a model we shall use the 0.39 cm cell for which actual data are listed in Table II. For the present purpose we may assume that radiant energy is absorbed uniformly throughout the gas and that the eventual temperature rise takes place at constant volume.

Table V. Product Ratio as a Function of T_m for 60 Torr of CClF_3 Irradiated at 1090 cm^{-1}

No.	E_{abs}/R , °K	T_{osc}^a , °K	T_m , °K	CPF, ^b %	$P_{\text{CF}_4}/P_{\text{C}_2\text{F}_6}$
1	9340	10100	1220	1.5 ₈	4.9
2	6840	7600	999	0.37 ₄	1.8
3	6040	6790	938	0.12 ₀	0.76
4	4240	4980	758	0.006 ₀	0.10

^a Equation 6. ^b $\ln(\text{CPF}) = (5.8 \pm 0.4) - (105.9 \pm 7.1)/(RT_{\text{osc}})$; $r = 0.990$. $\ln(\text{CPF}) = (9.7 \pm 0.9) - (22.0 \pm 1.8)/(RT_m)$; $r = 0.983$.

The laser-induced reactions of CCl_3F are summarized by the equation, $\text{CCl}_3\text{F} \rightarrow \frac{1}{2}\text{C}_2\text{Cl}_2\text{F}_2 + \text{Cl}_2$; $\Delta H^\circ = +30$ kcal. Thus, for experiment No. 5 in Table II, the endothermicity of the laser-induced reactions is $0.028 \times 30 = 0.8$ kcal/mol. On subtracting this from E_{abs} , we find that net energy available for heating the gas is 12.4 kcal/mol. Using data listed in the JANAF Tables,²⁰ the maximum temperature reached by the gas is calculated to be 903 K.

In the presence of H_2 , the reaction, $\text{CCl}_3\text{F} + \text{H}_2 \rightarrow \frac{1}{2}\text{C}_2\text{Cl}_2\text{F}_2 + 2\text{HCl}$, has $\Delta H^\circ = -14$ kcal. Thus, for experiment No. 9 in Table II, the maximum temperature reached by the H_2 -containing reaction mixture is found to be 984 K.

Finally, for the laser-induced reactions of CClF_3 , we shall represent the thermochemistry by the equation, $\text{CClF}_3 \rightarrow \frac{1}{2}\text{C}_2\text{F}_6 + \frac{1}{2}\text{Cl}_2$; $\Delta H^\circ = +9$ kcal. Thus, for experiment No. 1 in Table II, the maximum temperature reached by the reaction mixture is found to be 1220 K.

It is of interest to examine the timing of events subsequent to the laser flash. The primary process appears to take place while the absorbed energy is still largely in the mode into which it was originally introduced. The rate-limiting step for conversion of the absorbed energy into random thermal energy is V–T transfer,² which for fluorochloromethanes,²⁷ when extrapolated to our experimental conditions, proceeds with relaxation times on the order of 200–400 ns. Thus the laser-induced temperature jump of the gas phase will be nearly complete in about $1\ \mu\text{s}$.

The subsequent temperature drop by normal mechanisms of heat loss to the surroundings will be much slower. We have made explicit calculations only for the 0.39-cm cell and experiment No. 1, Table II, in which the maximum temperature T_m reaches to 1220 K. On solving the differential equation of thermal conduction for the given boundary conditions,²⁸ and using a value of $0.94\text{ cm}^2\text{ s}^{-1}$ for the thermometric conductivity (k/C_p),²⁹ we find that the mean temperature drop for the central 90% of the gas (i.e., all but the 10% immediately adjacent to the optical windows) is $0.9\text{ }^\circ\text{C}$ in $50\ \mu\text{s}$ and $5.5\text{ }^\circ\text{C}$ in $100\ \mu\text{s}$. For the concomitant temperature drop by radiation, we calculate $1.2\text{ }^\circ\text{C}$ in $50\ \mu\text{s}$ and $2.4\text{ }^\circ\text{C}$ in $100\ \mu\text{s}$, using a plausible upper limit of 0.1 for the emittance of CClF_3 .²⁹ These effects are statistically insignificant compared to the $\pm 90\text{ }^\circ\text{C}$ possible error in T_m resulting from 10% error in actinometry. Thus, for practical purposes, we may assume that subsequent to the rapid rise, the temperature remains essentially at T_m during the critical period, on the order of 10–100 μs , during which practically all the chemistry subsequent to the primary decomposition takes place.

For the 0.39-cm cell, return of the temperature of the gas phase to room temperature is practically complete within 0.2 s, which is short compared to the 3-s period between laser flashes. Thus, at the start of each flash, the gas is essentially at room temperature.

In the larger cell used for synthesis experiments, the absorbed energy density after the laser flash varies considerably

along the optical path. This results in temperature and pressure gradients and leads to turbulence and shock waves. However, even under these conditions the temperature of the gas near the front window, where most of the chemistry takes place, should remain close to the local T_m for 20–30 μ s. The rate of cooling after onset of turbulence is hard to estimate. However, return of the gas to room temperature between laser flashes seems to be reasonably complete. We never perceived more than mild warming, even after 1000 flashes.

Photochemistry vs. High-Temperature Chemistry. The preceding analysis leads to the following *idealized model* for megawatt-power infrared laser chemistry. (1) The primary process takes place while most of the excitation energy still resides in the specific vibrational mode that has been excited. This is photochemistry. (2) There is a rapid temperature jump as the excitation energy is degraded into random thermal energy. A maximum temperature T_m , potentially well above 1000 K, is reached. (3) The secondary reaction steps take place essentially at the temperature T_m . This is high-temperature chemistry. (4) The gas phase cools down to room temperature prior to application of the next laser flash.

This model is realistic enough to be useful and simple enough to permit ready interpretation of the chemistry. For instance, Table V compares the photochemically significant temperatures E_{abs}/R and T_{osc} with T_m , and lists relative yields of $\text{CF}_4/\text{C}_2\text{F}_6$ produced by irradiating CClF_3 as a function of these variables. CF_4 is formed by fluorine-abstraction (R4), for which an activation energy of 20 ± 10 kcal may be estimated, while C_2F_6 is formed by CF_3 radical combination with $E_{\text{act}} \approx 0$. Accordingly, the ratio of $[\text{CF}_4]/[\text{C}_2\text{F}_6]$ is expected to, and does, increase considerably with T_m .

Perhaps even more instructive are the very high values calculated for E_{abs}/R and T_{osc} , which range up to 10 000 K, while values of T_m range up to 1220 K. The former temperatures (particularly E_{abs}/R , as we have shown) can account for the activation energy of the primary process and for the fact that values of CPF are usefully high. We now wish to show that the alternative theory, that primary decomposition takes place *after* the temperature jump to T_m , is not tenable. The plot of $\ln(\text{CPF})$ vs. $(RT_m)^{-1}$ is adequately linear (Table V, footnote b), but the magnitude of the slope, 22 ± 2 kcal, is much too small to be identified with the activation energy for any conceivable decomposition process of CClF_3 .

Photochemical Efficiency. In conventional photochemistry one measures photochemical efficiency by the quantum yield. In high-power infrared laser chemistry there is no direct analogue to the quantum yield. However, one may define *photochemical efficiency* as the fraction of the absorbed energy which is utilized as activation energy. For instance, in line 1 of Table II, $E_{\text{abs}} = 18.6$ kcal and 1.58% of the molecules react. On introducing 86 kcal/mol for the activation energy, we find that the photochemical efficiency is $0.0158 \times 86/18.6$, or 0.073. Similarly, for the data listed in line 5 of Table II, the photochemical efficiency is 0.17; for the data listed in line 9, it is 0.83 if $E_{\text{act}} = 81$ kcal and >0.35 if part of the primary process proceeds via (R24). Compared with quantum yields in conventional photochemistry, these values are quite respectable.

The *energy efficiency* of infrared laser chemistry is distinctly greater than the photochemical efficiency because the absorbed laser energy is used twice: first to produce the photochemistry of the primary process, then to produce a high-temperature gas phase for subsequent reactions. This peculiar coupling of photochemistry with high-temperature chemistry should find many practical uses.

Acknowledgments. D.F.D. wishes to thank Mr. Gregory A. Hill for technical assistance during the experimental part of this investigation. E.G. wishes to thank Drs. Laurence I. Kleinman, Philip Keehn, and Hanns J. Wetzstein for numerous discussions. We warmly thank the officers of Brandeis University for encouraging basic research in spite of financial stringency.

References and Notes

- (1) (a) Work supported in part by a grant from the National Science Foundation; (b) Division of Natural Science, Macon Junior College, Macon, Ga. 31206; (c) John Simon Guggenheim Fellow.
- (2) N. V. Karlov, *Appl. Opt.*, **13**, 301 (1974).
- (3) J. T. Knudtson and E. M. Eyring, *Annu. Rev. Phys. Chem.*, **25**, 255 (1974).
- (4) R. N. Zitter, R. A. Lau, and K. S. Wills, *J. Am. Chem. Soc.*, **97**, 2578 (1975).
- (5) M. P. Freeman, D. N. Travis, and M. F. Goodman, *J. Chem. Phys.*, **60**, 231 (1974).
- (6) W. Braun, M. J. Kurylo, M. J. Kaldor, and R. P. Wayne, *J. Chem. Phys.*, **61**, 461 (1974).
- (7) M. J. Kurylo, W. Braun, A. Kaldor, S. M. Freund, and R. P. Wayne, *J. Photochem.*, **3**, 71 (1974).
- (8) A. Yoge and R. M. J. Benmair, *J. Am. Chem. Soc.*, **97**, 4430 (1975).
- (9) S. W. Mayer, M. A. Kwok, R. W. F. Gross, and D. C. Spencer, *Appl. Phys. Lett.*, **17**, 516 (1970).
- (10) (a) J. L. Lyman, R. J. Jensen, J. Rink, C. P. Robinson, and S. D. Rockwood, news release in *Science News*, **107**, 284 (1975); (b) R. J. Jensen et al., LASL Technical Report 87544, Los Alamos Scientific Laboratory, Los Alamos, N.M.
- (11) M. Lamotte, H. J. Dewey, R. A. Keller, and J. J. Ritter, *Chem. Phys. Lett.*, **30**, 165 (1975).
- (12) R. V. Ambartzumian and V. S. Letokhov, *Laser Focus*, **11** (No. 7), 48 (1975).
- (13) Experiments done at Brandeis University by S. P. Anderson, E. Grunwald, G. A. Hill, and P. Keehn, to be published.
- (14) G. Herzberg, "Infrared and Raman Spectra", Van Nostrand, New York, N.Y., 1945, p 314.
- (15) E. K. Plyler and W. S. Benedict, *J. Res. Natl. Bur. Stand.*, **47**, 202 (1951).
- (16) H. W. Thompson and R. B. Temple, *J. Chem. Soc.*, 1422 (1948).
- (17) R. B. Bernstein, J. P. Zietlow, and F. F. Cleveland, *J. Chem. Phys.*, **21**, 1778 (1953).
- (18) F. A. Jenkins and H. E. White, "Fundamentals of Physical Optics", McGraw-Hill, New York, N.Y., 1937, Section 18.1.
- (19) H. Babrov, G. Ameer, and W. Benesch, *J. Mol. Spectrosc.*, **3**, 185 (1959).
- (20) *Natl. Stand. Ref. Data Ser., Natl. Bur. Stand.*, **No. 37** (1971).
- (21) (a) J. D. Cox and G. Pilcher, "Thermochemistry of Organic and Organometallic Compounds", Academic Press, New York, N.Y., 1970; (b) S. W. Benson, "Thermochemical Kinetics", Wiley, New York, N.Y., 1968.
- (22) (a) V. N. Kondratiev, "Rate Constants of Gas Phase Reactions", translated by L. S. Holtzschlag, National Technical Information Service, Springfield, Va., 1972; (b) D. C. Nonhebel and J. C. Walton, "Free-Radical Chemistry", Cambridge University Press, Cambridge, England, 1974, Chapter 8.
- (23) (a) Insertion of real or virtual dihalocarbenes into various bonds has been discussed by D. Seyferth, "Carbenes", Vol. 2, R. A. Moss and M. Jones, Jr., Ed., Wiley-Interscience, New York, N.Y., 1975, Chapter 3. (b) The thermochemistry of CClF_3 is different from that of CF_2 . While CF_2 appears to react by direct dimerization (A. P. Modica, *J. Chem. Phys.*, **46**, 3663 (1967)), the "hot" $\text{C}_2\text{Cl}_2\text{F}_2$ molecules produced by direct combination of 2CClF_3 have enough energy to decompose exothermically to $\text{C}_2\text{F}_2 + \text{Cl}_2$. We find no compelling evidence that C_2F_2 is formed under our conditions.
- (24) (a) A. H. Sehon and M. Szwarc, *Proc. R. Soc. London, Ser. A*, **209**, 110 (1951). (b) For the analogous reaction, $\text{CF}_2\text{HCl} \rightarrow \text{CF}_2 + \text{HCl}$, $\Delta H^\circ_{298} = 51$ kcal, $E_{\text{act}} = 56$ kcal [J. W. Edwards and P. A. Small, *Nature (London)*, **202**, 1329 (1964)], $E_{\text{act}} = 51$ kcal [F. Gozzo and C. R. Patrick, *Nature (London)*, **202**, 80 (1964)], $E_{\text{act}} = 56$ kcal [G. R. Barnes, R. A. Cox, and R. F. Simmons, *J. Chem. Soc. B*, 1176 (1971)].
- (25) We are assuming effective cross sections comparable to those measured for V-V energy transfer of HF by R. M. Osgood, P. B. Sackett, and A. Javan, *J. Chem. Phys.*, **60**, 1464 (1974).
- (26) Rice-Ramsperger-Kassel-Marcus. For a recent review, see P. J. Robinson and K. A. Holbrook, "Unimolecular Reactions", Wiley, New York, N.Y., 1972.
- (27) R. C. Amme and S. Legvold, *J. Chem. Phys.*, **30**, 163 (1959); **33**, 91 (1960).
- (28) I. S. Sokolnikoff and E. S. Sokolnikoff, "Mathematics for Engineers and Physicists", 2d ed, McGraw-Hill, New York, N.Y., 1941, pp 369–375.
- (29) R. C. L. Bosworth, "Heat Transfer Phenomena", Wiley, New York, N.Y., 1952, pp 17, 29, and 46.